CHyCle 2017

sciforum

Conference Proceedings Paper

Satellite-observed solar-induced fluorescence to monitor global plant stress

Brianna R. Pagán[1*], Brecht Martens[1], Wouter H. Maes[1], Diego G. Miralles[1]

Published: 10/11/2017
Academic Editor: Sergio Vicente-Serrano

[1] Laboratory of Hydrology and Water Management, Ghent University; brianna.pagan@ugent.be, brecht.martens@ugent.be, wh.maes@ugent.be, diego.miralles@ugent.be
* Correspondence: brianna.pagan@ugent.be; Tel.: +32 9 264 61 40

Abstract: Biophysical feedbacks on climate depend on plant responses to stress conditions. Yet current land surface models (LSMs) still treat plant stress rudimentarily, and typically assume the same sensitivity to soil moisture for all vegetation types. There is a need therefore to investigate the dynamics of vegetation stress at the global scale, both to further understand the effect of land feedbacks on climate, as well as to improve the representation of these processes in LSMs. Here, we explore an index of evaporative stress (i.e. the ratio of actual to potential evaporation) based on satellite solar-induced fluorescence (SIF) observations, and we compare it to the estimates of evaporative stress by various LSMs from the eartH2Observe database. Results of validations against *in situ* evaporative stress – calculated from the FLUXNET2015 eddy-covariance archive – indicate that the SIF-based stress index outperforms the estimates of the LSMs across the majority of sites, with the exception of regions with sparse vegetation in which bare soil evaporation dominates the flux of vapour from land to atmosphere. This innovative SIF application can be used to further understand land–atmosphere feedbacks from different ecosystem types.

Keywords: solar-induced fluorescence; evaporative stress; transpiration

1. Introduction

Stomatal closure is regulated by plants to optimize water and carbon dioxide exchanges [1-3]. The proficiency of this optimization is contingent on plant species and environmental conditions such as temperature, radiation and water availability. Current land surface models (LSMs) typically parameterize these stressors and introduce dimensionless plant stress factors as multiplicative to net photosynthesis, stomatal conductance, potential transpiration, or other physical vegetation processes [e.g. 4-6]. In the case of water stress, the corresponding stress factor in LSM is often referred to as β. Some authors also refer to evaporative stress (S) in the context of evaporation, which when referred to transpiration may involve phenological controls other than water stress (see e.g. [7]). These multiplicative factors typically range from 0 (maximum stress) to 1 (minimum stress), and are commonly a function of normalized soil moisture (θ) standardized between field capacity (θ_{fc}) or critical point (θ_c) and wilting point (θ_{wp}). Functions used to represent the response of these factors to declines in soil moisture range from linear to highly nonlinear depending on the model (Figure 1) – (see also e.g. [8]). The numerous influencers on vegetation health make modeling of stress factors and their subsequent impact on transpiration and photosynthesis difficult, and the lack of global observations prevents exhaustive validation testing.

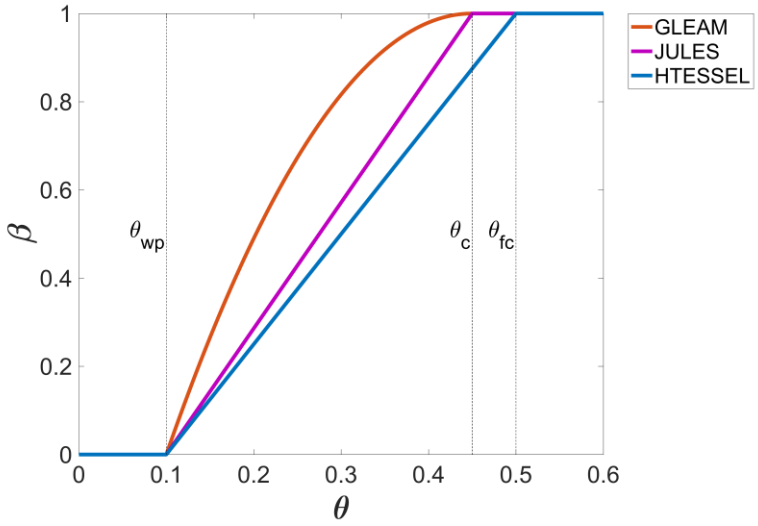

Figure 1. Examples of various models β response functions to declines in soil moisture. Theoretical values are used for θ_{fc}, θ_c and θ_{wp}.

Solar-induced fluorescence (SIF) is a subtle glow of energy emitted by vegetation during photosynthesis [9]. Recently, satellite observations of SIF have been shown to closely mimic the spatiotemporal variability of photosynthesis [10] and can constrain gross primary production measurements [11]. Given the nexus between photosynthesis and transpiration through stomatal regulation, a link between SIF observations and evaporative stress can be hypothesised. Here we use normalized SIF data as a proxy of *S*, understood as the ratio of actual over potential evaporation, and present the principal *in situ* validation dataset of stress across FLUXNET towers following the methodology presented in Maes et al [*in review*, 12]. The *S* estimates from three LSMs and one evaporation retrieval model from the eartH2Observe database (http://www.earth2observe.eu) are also compared against FLUXNET tower derived stress to better contextualize the potential improvements that SIF may provide for monitoring evaporative stress and transpiration.

2. Experiments

2.1 Data

SIF measurements are taken from the European Organisation for the Exploitation of Meteorological Satellites (EUMESTAT) Meteorological Operational Satellite-A (MetOp-A) using the Köhler et al., 2015 [13] retrieval method for the period 2007–2014 at 0.5° resolution. Data is subsequently temporally gapfilled to daily scale and smoothed using a 15-day moving window, and standardised as defined in Pagan et al. [*in review*, 14]. Data from three LSMs (Hydrology Tiled European Centre for Medium-Range Weather Forecasts (ECMWF) Scheme for Surface Exchanges over Land – Catchment-based Macro-scale Floodplain model; HTESSEL-CaMa, Joint United Kingdom Land Environment Simulator; JULES and Organising Carbon and Hydrology in Dynamic Ecosystems; ORCHIDEE) and one evaporation retrieval algorithm (Global Land Evaporation Amsterdam Model; GLEAM) is taken from the eartH2Observe database for 2007–2014 at 0.25° resolution. Three models (GLEAM, HTESSEL and ORCHIDEE) provide actual (E_a) and potential evaporation (E_p), thus stress can be estimated by:

$$S = E_a/E_p \quad (1)$$

In the case of JULES, S is not computed since E_P is not available, thus β is issued instead, which is derived by JULES as shown in Figure 1. Therefore, the S in JULES considers here only incorporates the effect of water stress, while for the other models it may incorporate other stress factors depending on their own definition of E_P. All other models from the eartH2Observe initiative are excluded due to E_P nor β being outputted. A summary of evaporation calculations used by each model and subsequent stress formulation used for this analysis can be found in Table 1.

Table 1. Evaporation and stress calculation schemes for each implemented eartH2Observe model.

Model	Evaporation	Stress
GLEAM [15]	Priestley and Taylor	$S = \frac{E_a}{E_p}$
HTESSEL-CaMa [16-17]	Penman-Monteith	$S = \frac{E_a}{E_p}$
JULES [5]	Penman-Monteith	$S = \beta = \begin{matrix} 1 & \theta \geq \theta_c \\ \frac{\theta - \theta_{wp}}{\theta_c - \theta_{wp}} & \theta_{wp} < \theta < \theta_c \\ 0 & \theta \leq \theta_{wp} \end{matrix}$
ORCHIDEE [18]	Bulk PET [19]	$S = \frac{E_a}{E_p}$

2.2 Validation

Data from the FLUXNET2015 archive (http://fluxnet.fluxdata.org/data/fluxnet2015-dataset/) is used to create an in situ evaporative stress validation dataset [12]. Stress is defined as the ratio of E_a to E_P (same as Eq. 1) for flux towers where E_P is estimated by a subset of unstressed days as outlined in Maes et al [12]. After masking for rain and snow using daily data from Multi-Source Weighted-Ensemble Precipitation (MSWEP v2.0) [20] and the European Space Agency (ESA) GLOBSNOW product [21], a minimum of 100 flux tower observations are required for each tower to remain in the comparison. Data from towers located in the same 0.5° pixel from the SIF grid are averaged. After masking, a total of 29 FLUXNET towers are used for the analysis.

3. Results

SIF derived stress outperforms all models in the comparisons to in situ S with the highest average correlation (0.68) amongst flux towers (Figure 2a). The correlation for the SIF derived stress factor ranges from 0.08 for Au-Wom to 0.95 for US-MMS. Au-Wom represents an outlier and exhibits low performance across all models, likely due to the atypical dynamics of the evaporative stress in this site. HTESSEL (0.55) and GLEAM v3a (0.14) follow in terms of mean performance, while JULES and ORCHIDEE exhibit average correlations close to zero. Nonetheless, the lower performance from JULES can be expected, as its stress factor only reflects soil moisture conditions and does not consider other potential constraints that may lead to differences between the actual land supply and the atmospheric demand for water, such as heat stress, low temperatures or vegetation leaf-out.

The cross correlations between each S estimate and the flux towers S are calculated for each site using lags of +/- 6 months. The lag of the highest cross-correlation is shown in Figure 2b. For the

overwhelming majority of sites, the SIF-based estimates are capable of capturing the seasonal cycle of evaporative stress from the in situ sites, as evidenced by the highest correlations being exhibited at zero lag. On the other hand, JULES demonstrates a clear delay in stress response ranging from 1-4 months, while ORCHIDEE exhibits a mixed signal, with lags in either direction.

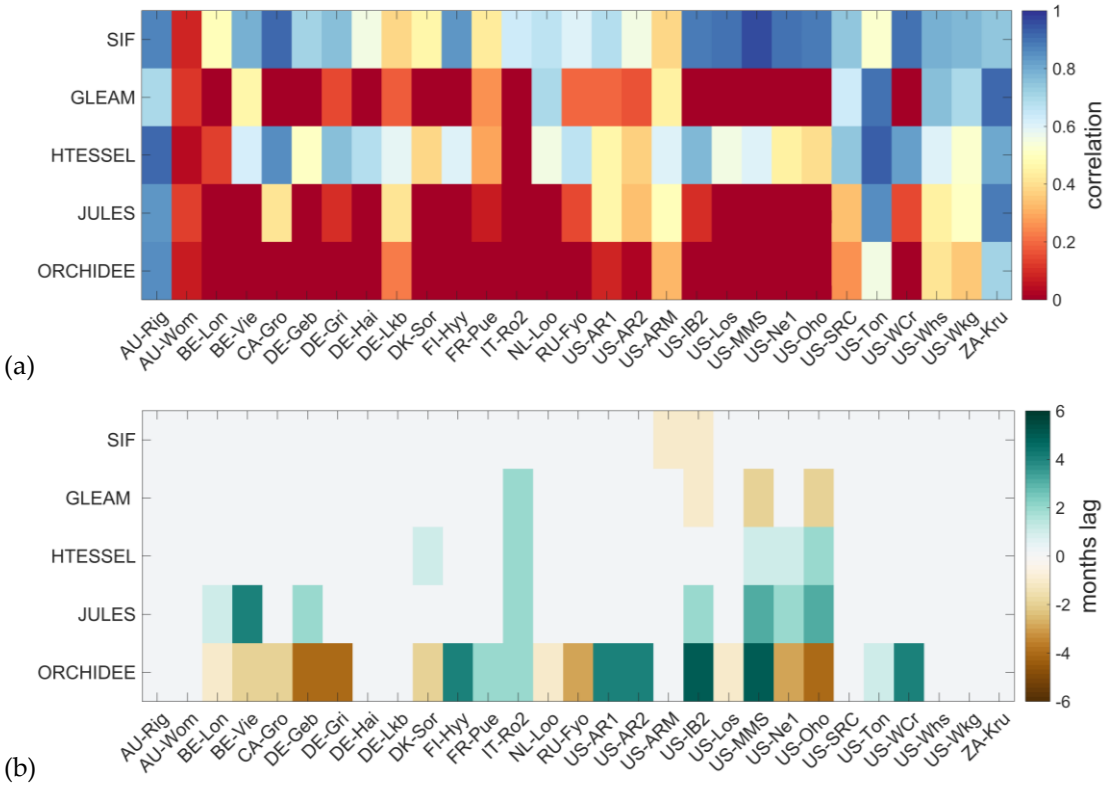

Figure 2. (a) Correlations of SIF-based and model-based S versus the tower estimates at 29 flux sites. (b) Lag (number of months) in which the cross-correlation is maximised.

4. Discussion

Since the SIF-derived *S* is only a measure of the evaporative stress of the vegetated fraction within the satellite footprint, its performance as evaporative stress indicator is overall lower in regions (e.g. US-Whs with over 50% bare soil). The LSMs include bare soil evaporation calculations, and commonly weight pixels based on fractions of vegetated area, explaining the improved performance for certain models relative to the SIF-based estimates over towers in regions with sparse or no vegetation. The analysed LSMs exhibit issues in capturing the seasonality of evaporative stress, either due to a too early or late wetting or drying. The SIF-derived stress appears to effectively capture this seasonality.

5. Conclusions

Overall, SIF-derived evaporative stress shows higher correlations against flux tower estimates than the analysed LSMs. Therefore, SIF can potentially be used to capture the heterogeneous response of vegetation to stress factors without numerous parameterizations, resulting in an observational and accurate representation of evaporative stress. The implications of this research are relevant to (a) the hydrology and climate modelling communities, given the opportunity to utilize our SIF-based evaporative stress to benchmark model representation of the land control over the atmospheric demand for water, and (b) the remote sensing community, that will see how an observation originally intended for the study of the carbon cycle is valorized through its application to study water cycle dynamics.

Acknowledgments: This work is funded by the European Research Council (ERC) under grant agreement n° 715254 (DRY–2–DRY) and the Belgian Science Policy Office (BELSPO) in the framework of the STEREO III project SR/02/329 (STR3S). B.R.P. acknowledges partial funding from the United States Department of Agriculture (USDA) and Water Resource and Policy Initiative's (WRPI) Water Resources Fellowship.

Author Contributions: D.G.M. and B.R.P. conceived and designed the experiments; B.R.P. performed the experiments and analysed the data; B.M. and W.H.M. contributed to the methods and analysis; all authors contributed to writing the paper.

Conflicts of Interest: The authors declare no conflict of interest.

Abbreviations

The following abbreviations are used in this manuscript:
CaMa: Catchment-based Macro-scale Floodplain model
EMCWF: European Centre for Medium-Range Weather Forecasts
EUMESTAT: European Organisation for the Exploitation of Meteorological
ESA: European Space Agency
GLEAM: Global Land Evaporation Amsterdam Model
HTESSEL: Hydrology Tiled ECMWF Scheme for Surface Exchanges over Land
JULES: Joint United Kingdom Land Environment Simulator
LSM: land surface model
Met-OpA: Meteorological Operational Satellite-A
MSWEP: Multi-Source Weighted-Ensemble
ORCHIDEE: Organising Carbon and Hydrology in Dynamic Ecosystems
SIF: solar-induced fluorescence

References

1. Collatz, G. J., Ball, J. T., Grivet, C., & Berry, J. A. (1991). Physiological and environmental regulation of stomatal conductance, photosynthesis and transpiration: a model that includes a laminar boundary layer. Agricultural and Forest Meteorology, 54(2–4), 107–136. https://doi.org/10.1016/0168-1923(91)90002-8.
2. Cowan, I. R., & Farquhar, G. D. (1977). Stomatal function in relation to leaf metabolism and environment. Symposia of the Society for Experimental Biology, 31(1973), 471–505. https://doi.org/0081-1386.
3. Tardieu, F., & Simonneau, T. (1998). Variability among species of stomatal control under fluctuating soil water status and evaporative demand: modelling isohydric and anisohydric behaviours. Journal of Experimental Botany, 49(Special), 419–432. https://doi.org/10.1093/jxb/49.Special_Issue.419.
4. Arora, V. K. (2003). Simulating energy and carbon fluxes over winter wheat using coupled land surface and terrestrial ecosystem models. Agricultural and Forest Meteorology, 118(1–2), 21–47. https://doi.org/10.1016/S0168-1923(03)00073-X.
5. Best, M. J., Pryor, M., Clark, D. B., Rooney, G. G., Essery, R. L. H., Ménard, C. B., … Harding, R. J. (2011). The Joint UK Land Environment Simulator (JULES), Model description – Part 1: Energy and water fluxes. Geoscientific Model Development Discussions, 4(1), 595–640. https://doi.org/10.5194/gmdd-4-595-2011.
6. Boussetta, S., Balsamo, G., Beljaars, A., Panareda, A. A., Calvet, J. C., Jacobs, C., … Van Der Werf, G. (2013). Natural land carbon dioxide exchanges in the ECMWF integrated forecasting system: Implementation and offline validation. Journal of Geophysical Research Atmospheres, 118(12), 5923–5946. https://doi.org/10.1002/jgrd.50488.
7. Miralles, D. G., Holmes, T. R. H., De Jeu, R. A. M., Gash, J. H., Meesters, A. G. C. A., & Dolman, A. J. (2011). Global land-surface evaporation estimated from satellite-based observations. Hydrology and Earth System Sciences, 15(2), 453–469. https://doi.org/10.5194/hess-15-453-2011.
8. Powell, T. L., Galbraith, D. R., Christoffersen, B. O., Harper, A., Imbuzeiro, H. M. A., Rowland, L., … Moorcroft, P. R. (2013). Confronting model predictions of carbon fluxes with measurements of Amazon forests subjected to experimental drought. New Phytologist, 200(2), 350–365. https://doi.org/10.1111/nph.12390.

9. Papageorgiou, G. (1975). Chlorophyll fluorescence: an intrinsic probe of photosynthesis. Bioenergetics of Photosynthesis, 319–371.
10. Guanter, L., Zhang, Y., Jung, M., Joiner, J., Voigt, M., Berry, J. A., … Griffis, T. J. (2014). Global and time-resolved monitoring of crop photosynthesis with chlorophyll fluorescence. Proceedings of the National Academy of Sciences of the United States of America, 111(14), E1327-33. https://doi.org/10.1073/pnas.1320008111.
11. Zhang, Y., Xiao, X., Jin, C., Dong, J., Zhou, S., Wagle, P., … Zhang, G. (2016). Consistency between sun-induced chlorophyll fluorescence and gross primary production of vegetation in North America. Remote Sensing of Environment, 183, 154–169.
12. Maes W. H., Gentine, P., Verhoest, N., & Miralles, D. G. Potential evaporation at eddy-covariance sites across the globe. *in review*.
13. Köhler, P., Guanter, L., & Joiner, J. (2015). A linear method for the retrieval of sun-induced chlorophyll fluorescence from GOME-2 and SCIAMACHY data. Atmospheric Measurement Techniques, 8(6), 2589–2608. https://doi.org/10.5194/amt-8-2589-2015.
14. Pagán, B. R., Martens, B., Maes, W. H., Gentine, P., Miralles, D. G. Global evaporative stress from solar-induced fluorescence. *in review.*
15. Martens, B., Miralles, D. G., Lievens, H., van der Schalie, R., de Jeu, R. A. M., Férnandez-Prieto, D., … Verhoest, N. E. C. (2016). GLEAM v3: satellite-based land evaporation and root-zone soil moisture. Geoscientific Model Development Discussions, (August), 1–36. https://doi.org/10.5194/gmd-2016-162.
16. Balsamo, G., Beljaars, A., Scipal, K., Viterbo, P., van den Hurk, B., Hirschi, M., & Betts, A. K. (2009). A revised hydrology for the ECMWF model: Verification from field site to terrestrial water storage and impact in the Integrated Forecast System. Journal of Hydrometeorology, 10(3), 623–643.
17. Yamazaki, D., Kanae, S., Kim, H., & Oki, T. (2011). A physically based description of floodplain inundation dynamics in a global river routing model. Water Resources Research, 47(4).
18. D 'orgeval, T., Polcher, J., & De Rosnay, P. (2008). Sensitivity of the West African hydrological cycle in ORCHIDEE to infiltration processes. Hydrol. Earth Syst. Sci, 12, 1387–1401. Retrieved from www.hydrol-earth-syst-sci.net/12/1387/2008/.
19. Barella-Ortiz, A., Polcher, J., Tuzet, A., & Laval, K. (2013). Potential evaporation estimation through an unstressed surface-energy balance and its sensitivity to climate change. Hydrology and Earth System Sciences, 17(11), 4625–4639. https://doi.org/10.5194/hess-17-4625-2013.
20. Beck, H. E., Van Dijk, A. I. J. M., Levizzani, V., Schellekens, J., Miralles, D. G., Martens, B., & De Roo, A. (2017). MSWEP: 3-hourly 0.25° global gridded precipitation (1979-2015) by merging gauge, satellite, and reanalysis data. Hydrology and Earth System Sciences, 21(1), 589–615. https://doi.org/10.5194/hess-21-589-2017.
21. Luojus, K., Pulliainen, J., Takala, M., Lemmetyinen, J., Kangwa, M., Smolander, T., & Derksen, C. (2013). Global snow monitoring for climate research: Algorithm Theoretical Basis Document (ATBD)–SWE-algorithm. In Technical Report.